Optical cooling of atomic hydrogen in a magnetic trap

T. W. Hijmans and O. J. Luiten

Natuurkundig Laboratorium, Universiteit van Amsterdam, Valckenierstraat 65/67, 1018 XE Amsterdam, The Netherlands

I. D. Setija and J. T. M. Walraven

Van der Waals Laboratorium, Universiteit van Amsterdam, Valckenierstraat 65/67, 1018 XE Amsterdam, The Netherlands

Received April 5, 1989; accepted June 19, 1989

We describe the prospects for optical cooling of magnetically trapped atomic hydrogen. We analyze the performance of an optical system currently under development in our laboratory and present calculations for the optical cooling rate. We conclude that by using optical techniques hydrogen can be cooled to below 10 mK while the density is simultaneously boosted to approximately 10^{14} cm^{-3}. The same system can be used for thermometry down to temperatures well into the microkelvin regime.

1. INTRODUCTION

At first the hydrogen atom (H) seems to be a textbook candidate for optical cooling experiments. Under suitable conditions H can be spin polarized, thus virtually eliminating recombination to the molecular state. Unlike any other atomic or molecular system, atomic H remains gaseous down to 0 K, which makes the system an ideal testing ground for the investigation of fundamental quantum properties. One of the most dramatic manifestations of these quantum effects would undoubtedly be the observation of Bose–Einstein condensation (BEC) in H. Despite many efforts, no one has yet succeeded in reaching the conditions necessary for the occurrence of BEC, a combination of high density and low temperature, but along the way many important results concerning the condensed-matter aspects of H gas have been obtained. In practice, recombination to the molecular state both in the gas phase and on surrounding surfaces puts a practial limit on the maximum achievable densities, $n < 5 \times 10^{18}$ cm^{-3}. For a summary of a variety of experimental results, the reader is referred to some recent review papers.[1,2]

From a spectroscopic point of view H clearly stands out as the most simple and well-understood system. It remains one of the most valuable systems for the study of fundamental quantum-physical problems, thus it is no surprise that both atomic and condensed-matter physicists are eager to apply optical cooling techniques to this unique system.[3,4] However, this is not easily done owing to the awkward wavelength (121.6 nm) of the $1S$–$2P$ Lyman-α (Ly-α) transition. To date no optical cooling of H has been performed. In this paper we describe and analyze the way in which we are trying to approach this problem. The method is specifically tailored to suit our interest in the condensed-matter aspects of atomic H. It is applicable to relatively high densities of atoms (up to 10^{14} cm^{-3}) that are precooled to temperatures below 0.4 K and confined in a magnetic trap. Different schemes, with other applications in mind, have been proposed by other authors.[3] In addition to optical cooling, we plan to use optical techniques for thermometry and detection of the atoms under conditions in which other methods lack sensitivity.

2. OPTICAL SETUP

The chief obstacle facing potential optical coolers of H is the necessity of using pulsed schemes to generate VUV Ly-α radiation of sufficient intensity. In order to reach temperatures close to the Doppler limit (2.4 mK for H), the bandwidth of the light has to be comparable with the natural linewidth of the transition (100 MHz). According to the Fourier theorem this requires relatively long pulses. In order to achieve the smallest bandwidth, we opted for a system based on pulsed amplification of narrow-band cw radiation. In Fig. 1 we show a schematic of this system. The cw part consists of an Ar^+-pumped (Coherent Innova 200-15) single-mode ring dye laser (Coherent 699-21) operating at a wavelength of 730 nm. This light is amplified in three stages in a pulsed dye amplifier (Lambda Physik 2003) pumped by an excimer laser (Lambda Physik LPX 210i) and is then frequency doubled in a KDP crystal. The ensuing 365-nm light is amplified once more by the remaining part of the excimer beam. The pump laser produces pulses of 400-mJ energy and 25-nsec duration at a maximal repetition rate of 100 Hz. After three stages we obtained 730-nm pulses of 10–15 mJ and a near-transform-limited bandwidth of 30 MHz. After the second-harmonic generation (SHG) and the final amplification stage the pulse energy is 15–20 mJ, and the bandwidth 40 to 60 MHz. A similar system operating at a different frequency and without the amplification stage after the SHG crystal was used by Chu *et al.*[5] The 365-nm pulses will be used to produce Ly-α radiation by third-harmonic generation (THG) in a mixture of Ar and Kr.[6] This tripling cell is currently under construction. The UV intensity is sufficient to ensure a conversion efficiency of 10^{-6} to 10^{-5}, or 10^9 to 10^{10} Ly-α photons per pulse. The bandwidth in the VUV will be approximately 100–150 MHz, and a single Ly-α beam will be used for the cooling. Figure 2 shows a

0740-3224/89/112235-09$02.00

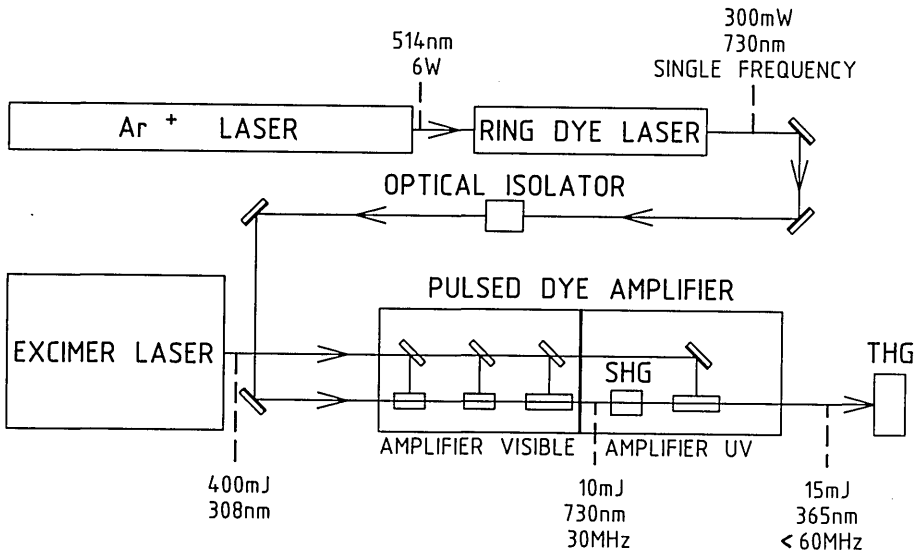

Fig. 1. Schematic of the optical setup.

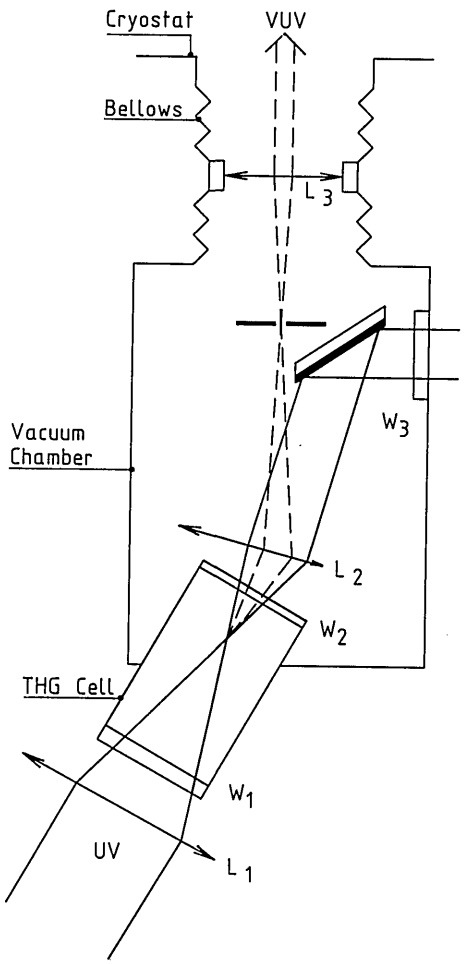

Fig. 2. Tripling cell and VUV monochromator. L_1, fused-silica lens; L_2 and L_3, MgF_2 lenses; W_1 and W_3; fused-silica windows; W_2, MgF_2 window. The beam width is expanded to unrealistic proportions for visual purposes.

schematic of the THG cell and the monochromator used to separate the VUV light from the large UV background. The fundamental and third-harmonic beams ensue from the THG cell as concentric cones. By exploiting the different refractive indices of MgF_2 for 365 and 121.6 nm, a MgF_2 lens that is placed off axis may be used to focus the Ly-α beam onto a small aperture while the fundamental beam is deflected away onto a beam dump. A similar monochromator was used by VonDrasek *et al.*[7]

The scheme described above yields an exceptionally small bandwidth but is unsuited for the usual optical-molasses[8] or beam-stopping[9,10] experiments owing to the relatively low repetition rate of the excimer laser: the atoms would simply escape in the time span between two pulses. This problem is eliminated when the atoms are confined in a magnetic trap. Magnetic confinement of spin-up-polarized hydrogen ($H\uparrow$) was proposed by Hess[11] and first demonstrated by Hess *et al.* at MIT.[12] Shortly thereafter a different trapping scheme was successfully applied by van Roijen *et al.*[13] Research related to the experiments that we propose here, optical cooling of magnetically trapped Na atoms, was carried out by Bagnato *et al.*[14] Since the analysis of the optical cooling of $H\uparrow$ depends in a crucial way on the geometry of the confinement field, we next briefly describe the trap used by van Roijen *et al.* We plan to use essentially the same trap for the optical experiments described in this paper.

3. MAGNETIC TRAP

In order to achieve wall-free confinement of $H\uparrow$, the magnitude of the magnetic field needs to show a minimum in free space. In the experiment of van Roijen *et al.* this was established with a combination of dipole and quadrupole magnets. The layout of the magnetic field profile is shown in Fig. 3. The axial field has a quadratic minimum $B_z = \alpha(z - z_0)^2 + \beta$. The transverse contribution due to the quadrupole coils increases linearly with distance from the axis at a slope γ. Van Roijen *et al.* used $\alpha = 0.1\ T/cm^2$, $\beta = 0.05$ T, and $\gamma = 2.2$ T/cm.[13] The finite value β of the field at the trap minimum not only serves to suppress Majorana (spin-flip) transi-

tions, which lead to loss of atoms from the trap, but will also spectrally separate different fine-structure components of the $1S$–$2P$ transition, which is essential for optical cooling experiments. For the latter reason we shall use a slightly higher value for β (0.1 T) in the calculations below. In the optical experiments a single Ly-α beam will enter the trapping region along the z direction. The H atoms are produced in a dissociator of the type pioneered by Hardy *et al.*,[15] which operates at 600 mK and is located in a field of 4.5 T. The low-field-seeking H↑ atoms are driven toward the field minimum by the field gradient and subsequently thermalize with the surrounding walls. Paradoxically, the collisions with the wall play an important role in establishing wall-free confinement. A single particle that enters a hypothetical trap without surrounding walls will never be confined, as it has no way of dissipating the kinetic energy it picks up as it accelerates toward the field minimum: the atom will career out of the trap. Although it is ultimately the atom–atom collisions that redistribute the energy among the particles and are thus responsible for establishing thermal equilibrium, the mean free path for these collisions is often larger than the dimensions of the trap. In this case the walls prevent the atoms from escaping and thus enable the attainment of high densities. In light of the above remarks, the term wall-free confinement should be interpreted somewhat loosely as referring to sufficient suppression of the density near the cell boundaries to eliminate surface-catalyzed recombination and relaxation processes. Another important feature of this confinement scheme is that the thermal equilibration time of the gas with the wall is substantially longer than the time needed for the gas to establish internal thermal equilibrium. After internal equilibration the spatial density distribution $n(r)$ of the gas in the trap will be a Boltzmann distribution $n(r) = n_0 \exp\{-\mu_B[B(r) - B(0)]/k_BT\}$. It is useful to define effective volumes of the sample by integrating m-particle distribution functions over the trap[13]:

$$V_{me} \equiv \int [n(r)/n_0]^m dr. \tag{1}$$

In particular,

$$n_0 \equiv N/V_{1e}, \tag{2}$$

where n_0 is the density at the center of the trap. The effective volumes V_{me} and the relation between n_0 and N depend on the geometry of the trap and have to be calculated numerically. For our trap we obtain approximately $V_{2e}T^{-5/2} = 6.4\ \mathrm{cm^3\ K^{-5/2}}$ and $V_{1e}T^{-5/2} = 34\ \mathrm{cm^3\ K^{-5/2}}$.

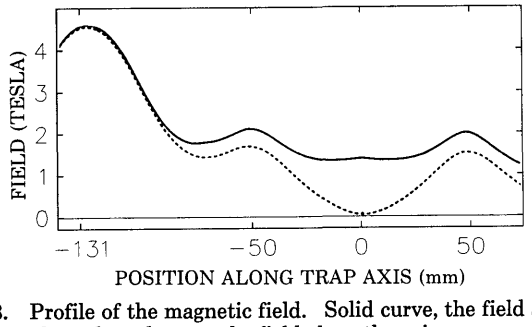

Fig. 3. Profile of the magnetic field. Solid curve, the field at the cell boundary; dotted curve, the field along the axis.

The role of atom–wall collisions constitutes an important difference between the trapping experiments performed in Amsterdam[13] and at MIT.[12,16] In the Amsterdam experiment the magnetic-field minimum was completely surrounded by walls, one of which served as the magnetic barrier at the loading side of the trap. By this last remark we mean that the magnetic potential barrier on this side of the trap is so high (4.5 T) that the atoms, once thermalized, have insufficient energy to climb the hill. Hence no low-field-seeking particles could escape. In contrast, the MIT trap contained a comparatively shallow magnetic barrier on one side of the sample cell over which particles could escape. The maximum attainable density during loading is determined by the balance of the flux of particles entering the trap and the two loss mechanisms, namely, relaxation to high-field-seeking atoms (H↓) and low-field-seeking atoms (H↑) escaping from the trap. The suppression of the latter mechanism in the Amsterdam experiment resulted in densities ($n_0 = 3 \times 10^{14}\ \mathrm{cm^{-3}}$) considerably higher than the values obtained at MIT ($n_0 = 5 \times 10^{12}\ \mathrm{cm^{-3}}$). On the other hand, the temperature in the Amsterdam experiment was limited by that of the apparatus (80 mK), while at MIT temperatures below 3 mK have been reached. This is because the particles escaping the trap over the barrier have a much higher than average energy, causing the remaining gas to cool to well below the wall temperature, an effect called evaporative cooling.

Owing to the absence of surface-catalyzed recombination the H↑ gas in a trap can be cooled to extremely low temperatures, but unfortunately the limited intrinsic stability of H↑ prevents the density from becoming larger than approximately $10^{15}\ \mathrm{cm^{-3}}$. At higher density the gas rapidly decays to high-field-seeking states through magnetic dipolar spin relaxation.[17,18] For the observation of many-body quantum effects such as BEC it is therefore imperative to combine low temperatures with the maximum density that can practically be attained. In this light the evaporative cooling technique seems disadvantageous when compared with optical cooling, since with the former technique atoms are intrinsically lost during the cooling process, while the optical method is in principle nondestructive. This drawback of evaporative cooling is, however, less serious than one would suspect: as was argued theoretically[11,19] and demonstrated experimentally,[16] the self-compression of the gas toward the center of the trap on cooling is sufficient to more than compensate for the loss of atoms. Therefore, in principle, it is possible to reach densities of more that $10^{14}\ \mathrm{cm^{-3}}$ with evaporation if one takes care not to increase the effective volume of the trap during the cooling. We have chosen to incorporate optical techniques for three reasons. First, since the number of atoms remains constant, the effect of self-compression on cooling is much greater than with evaporative methods, which allows one to start the cooling with samples of lower density ($5 \times 10^{11}\ \mathrm{cm^{-3}}$). This is important because the trap will necessarily be open, as in the MIT case, so one can gain optical access from one side and observe transmitted light at the other. Second, the introduction of optical techniques is indispensible for detecting H atoms at low temperatures, as other methods lack sensitivity. In Section 6 below we discuss these detection methods as well as a way to determine the temperature of the gas optically. The third rationale for attempting optical cooling of trapped H is

the physics of the cooling process itself, which differs in some respects from previously performed experiments. We first analyze the specific problems encountered when optically cooling trapped H and present some numerical calculations pertaining to the cooling process.

4. OPTICAL COOLING OF TRAPPED H

One may wonder if, even when a suitable optical transition is present, the use of a single pulsed beam of moderate repetition rate frustrates the cooling process. This is not the case, despite the fact that the light pressure is exerted on the gas only from one side and intermittently. There are three criteria to be fulfilled: (1) the interatomic collision rate must be sufficiently high to ensure that the gas establishes internal thermal equilibrium on a time scale short compared with the cooling rate, (2) the tuning of the source must be such that energy is extracted from the gas, and (3) the cooling must proceed sufficiently rapidly to overcome the minor heat leak to the walls. We should note that condition (1) is not stringent; even if the atoms do not collide at all, energy can still be extracted from the system since the orbit time of the particles in the trap (typically of the order of milliseconds) is short compared with the cooling rate. As the particles swing back and forth in the trap they still absorb light predominantly when they move toward the source if the detuning is negative. If we were to relax condition (1), the analysis would become complicated partly because of the spatial dependence of the resonance frequency in the trap and because the gas may be optically dense. These problems can be easily dealt with if thermal equilibrium is assumed. As long as condition (1) is consistent with conditions (2) and (3), it is in no way restrictive, as one can always reduce the Ly-α power to lower the cooling rate. The internal thermalization time τ_c due to elastic collisions is given by[13]

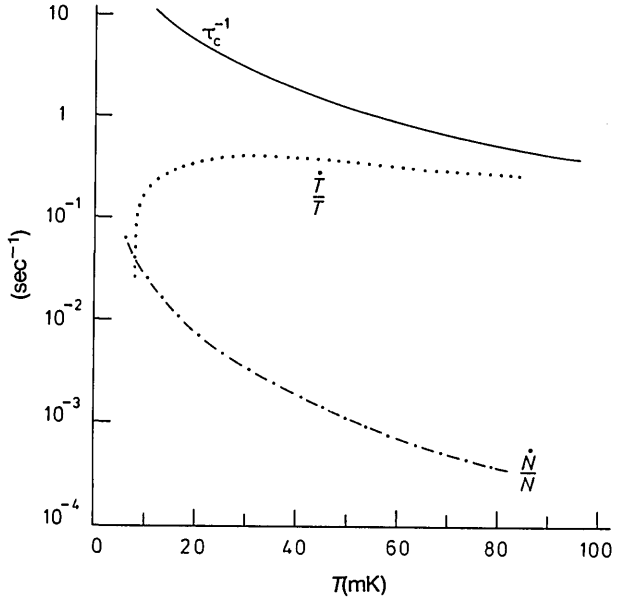

Fig. 4. Various relevant time constants calculated for 5×10^{10} atoms. τ_c, the internal equilibration time of the gas; $\dot{N}/N$, the characteristic decay time due to dipolar relaxation; $\dot{T}/T$, the cooling rate assuming a photon flux of 5×10^{11} sec^{-1}.

$$\tau_c^{-1} \approx \tfrac{1}{2} n_0 \bar{v}_r \sigma, \tag{3}$$

where $\bar{v}_r = (8k_BT/\pi\mu)^{1/2}$ is the average relative atomic speed (with μ the reduced mass of the scattering pair), $\sigma = 8\pi a^2$ is the scattering cross section for a pair of identical atoms with s-wave scattering length $a = 0.72$ Å, and $\zeta = V_{2e}/V_{1e} \approx 0.19$ is a constant determined by the geometry of our trapping field. The solid curve in Fig. 4 represents τ_c^{-1} versus the temperature for a fixed number $N = 5 \times 10^{10}$ atoms in the trap. This equilibrium rate increases at lower temperatures because the density increases as the gas becomes more confined near the center of the trap.

In contrast to τ_c, the gas–wall thermalization time τ_w depends on the density of atoms near the walls, a quantity that becomes exponentially small at low temperatures. To within a factor of order unity τ_w is given by[20]

$$\tau_w^{-1} = \tau_c^{-1} \exp(-\epsilon_{tr}/k_BT). \tag{4}$$

Here $\epsilon_{tr}/k_B = 0.92$ K represents the trap depth, where k_B is Boltzmann's constant. Even at 100 mK, τ_w is four orders of magnitude longer than τ_c. An additional criterion of practical importance is that the cooling has to proceed faster than the loss rate of atoms due to dipolar relaxation. For a given density of atoms in the center of our trap, the characteristic time for dipolar relaxation is given by[13]

$$\tau_r^{-1} \equiv -\dot{N}/N = \gamma_{dd} G_{dd} n_0 \zeta, \tag{5}$$

where G_{dd} is the dipolar rate constant evaluated at the center of the trap, and γ_{dd} is a factor that contains the effects of the inhomogeneous magnetic field through the field dependence of the rate. Below 100 mK the product $\gamma_{dd}G_{dd}$ is for our trap approximately equal to 2.5×10^{-15} cm^3/sec. As is the case for τ_c, the temperature dependence of τ_r scales with that of n_0. In addition to dipolar relaxation there is spin-exchange relaxation. The latter process does not affect pairs of atoms in the doubly polarized (electron- and nuclear-spin) hyperfine state. This state is denoted by d in Fig. 5. The c state contains some admixture of spin-down polarization, and atoms in this state are therefore susceptible to spin-exchange relaxation. Since the latter process is much faster, the c state is rapidly depleted, leaving a gas that is almost completely doubly polarized.[13] As long as the optical cooling rate $\dot{T}/T$ is larger than τ_r^{-1} and τ_w^{-1}, the gas of d atoms can be cooled with negligible loss of particles. In Fig. 4 we show a curve (the dotted curve) for this cooling rate at a photon flux of 5×10^{11} sec^{-1} (5×10^9 photons/pulse, 100-Hz repetition rate) calculated using a model presented below.

We now consider the effect of the tuning of the source frequency. This is not entirely trivial owing to two complicating effects: the inhomogeneity of the magnetic field and the consequent dependence of the resonance frequency of an atom on its location in the trap, and the fact that the density of the gas is so high that it is no longer an optically thin medium. A detailed evaluation of these effects requires numerical calculations that we present below. We limit ourselves first to a general discussion of the problem.

In Fig. 5 we show the energy levels of the $n = 2$ state of the H atom as well as those in the ground state. As mentioned above, only the d state is appreciably occupied. The allowed transitions from the d state to the $2P$ manifolds are denoted by arrows in Fig. 5 (the hyperfine splitting of the excited

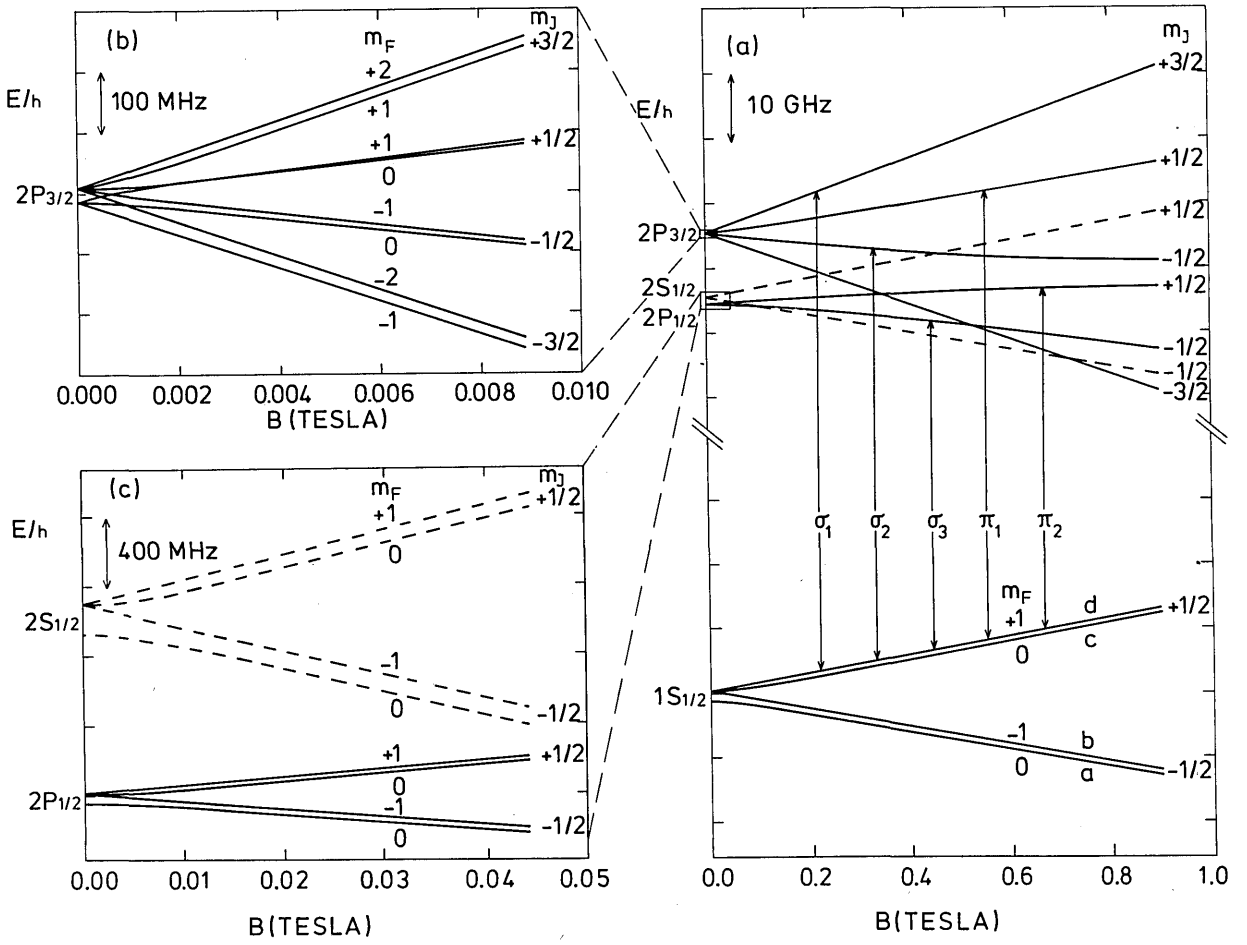

Fig. 5. Hyperfine-level diagram for the ground state and first excited state of H. (a) An overview; (b) and (c) exploded views of the $2P_{3/2}$ and the $2P_{1/2}$, $2S_{1/2}$ manifolds, respectively. The arrows denote the allowed optical transitions from the doubly polarized d levels of the ground-state manifold.

levels is too small to be resolved on this scale). For optical cooling it is essential that the excited state can only decay back to the original d state, otherwise the spin of the atom would be flipped after a few absorption–emission cycles and the atom would be expelled from the trap. The only transition that forms a closed cycle with the d state is the one to the $2P_{3/2}$ $m_F = 2$ level, denoted σ_1 in Fig. 5. The σ_1 transition has the additional advantage of having a positive gyromagnetic ratio. This implies that no atoms have a lower resonance frequency than those located at the position of the field minimum and that the inhomogeneous broadening manifests itself mainly on the blue side of the line while the Doppler broadening is noticeable chiefly on the red flank. In Fig. 6(a) we show the absorption spectrum of hydrogen gas with a density of 10^{11} cm^{-3} at the center of the trap calculated for two different temperatures. The difference in linewidth, which is due to a larger spatial extension of the sample at the higher temperature, is evident. In Fig. 6(b) the part of the spectrum near the σ_1 line is shown in more detail for $T = 0.1$ K. For comparison, a hypothetical spectrum that contains only inhomogeneous but no Doppler broadening is also shown. The difference between these two curves (the hatched area) is clearly most pronounced on the low-frequency side of the absorption line for the σ_1 transition. It is in this frequency region that the laser should be tuned to obtain the most efficient optical cooling. We should mention that the σ_1 transition has σ^+ polarization and σ_2 and σ_3 have σ^- polarization to the extent that the hyperfine interaction may be neglected in the excited state. We do not make use of this fact in our cooling scheme and in fact use unpolarized light. The only relevant parameter is the spectral separation between the σ_1 line and the closest other transition (π_1). This is entirely determined by the value of the field at the trap minimum. For $\beta = 0.1$ T the probability of exciting the π_1 transition when tuned for optimal cooling on the σ_1 line is less than 1%. This does not seem small, but for our purpose it is sufficient since only approximately 80 photons/atom are needed to cool down to the lowest attainable temperature. This high cooling efficiency is due to the large momentum of the Ly-α photon and the small mass of the H atom. Although some atoms may absorb more than 80 photons, thermal equilibrium implies that all atoms are cooled equally efficiently and hence the number of particles decreases by no more than a factor of 2 during the cooling process. By slightly increasing the value β of the field at the minimum, this already small loss mechanism can be almost completely suppressed.

Rather than calculating the optical cooling rate in terms of a semiclassical Langevin equation, as is often done to describe the cooling of neutral atomic beams,[21] we compute the average frequency difference of the incoming and scattered light in a similar way as is done by Wineland and Itano.[22]

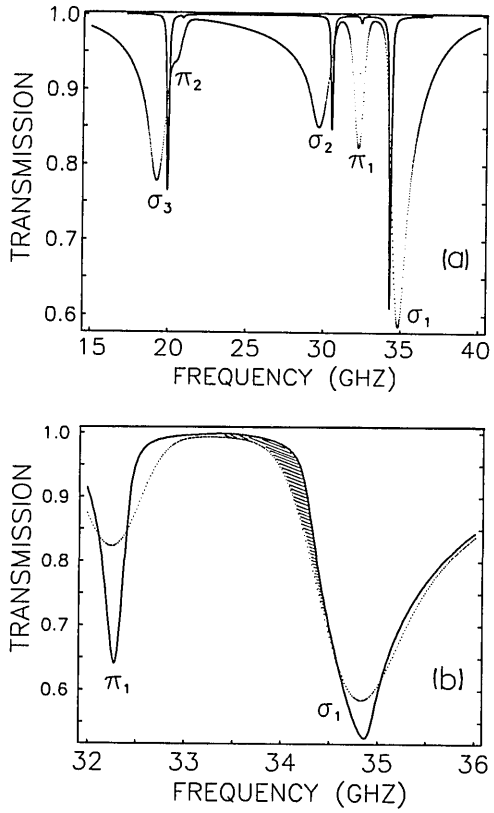

Fig. 6. (a) Calculated absorption spectrum of H in a magnetic trap at T = 100 mK (dotted curve) and T = 1 mK (solid curve). The calculation was performed assuming a density n_0 of 10^{11} cm^{-3} at the center of the trap and a beam diameter of 1 mm. The spectrum at T = 1 mK is enlarged by a factor of 10 for comparison. (b) Expanded view of the spectrum at 100 mK near the σ_1 line. The difference between the bare (solid curve) and Doppler-broadened (dotted curve) spectrum is denoted by the shaded area.

This quantity is proportional to the cooling rate as long as the gas remains in internal thermal equilibrium. The maximum cooling efficiency is obtained when the transition is driven at the brink of saturation,[21] i.e., for a saturation parameter $s \equiv \frac{1}{2}\omega_1^2/[(\Delta - \mathbf{k}_L \cdot \mathbf{v})^2 + \frac{1}{4}\Gamma^2] \approx 1$. Here ω_1 is the Rabi frequency, Γ is the natural linewidth, $\mathbf{k}_L$ is the wave vector of the incoming light, $\mathbf{v}$ is the velocity of the atom, and $\Delta \equiv \omega_L - \omega_0$ is the detuning. The angular frequency of the laser and the transition in the rest frame of the atom are denoted ω_L and ω_0, respectively. For a detuning of 200 MHz and 10-nsec pulses of 5×10^9 photons/pulse, the condition s = 1 corresponds to a beam radius of 0.2 mm, which is of the same order as the typical sample radius in the temperature range where optical cooling can be used. We therefore conclude that it is realistic to assume that the cooling can be performed under nearly optimal conditions, i.e., with s close to or slightly less than 1.

For $s < 1$, the differential elastic scattering cross section of a single atom is defined by

$$\frac{d^2\sigma(\omega_L, \omega_s)}{d\Omega d\omega_s} = C \frac{(\epsilon_s \cdot \mathbf{D}_{12})^2 (\epsilon_L \cdot \mathbf{D}_{21})^2}{[\omega_L - \omega_0 - \mathbf{k}_L \cdot \mathbf{v} - (\hbar k^2/2m)]^2 + \frac{1}{4}\Gamma^2} \times \delta(\omega_s - \omega_L + \mathbf{v} \cdot (\mathbf{k}_L - \mathbf{k}_s) + \hbar(\mathbf{k}_L - \mathbf{k}_s)^2/2m), \quad (6)$$

where $C = e^4\omega^4/16\pi^2\epsilon_0^2\hbar^2c^4$, ϵ denotes a polarization vector, m is the mass of the atom, and $\mathbf{D}_{21}$ is the dipole matrix elements between the ground (1) and exited (2) states in the rest frame of the atom. The subscript s refers to scattered light. We first consider optically thin samples, assuming uniform illumination. The average difference in frequency of a photon before and after scattering can be calculated from Eq. (6) by integrating over the solid angle Ω, averaging over the thermal velocity distribution and over the distribution $P(\omega_0)$ of values ω_0 associated with the inhomogeneous magnetic field, and dividing by the total-absorption cross section σ:

$$\langle \omega_s - \omega_L \rangle = \frac{\int d\omega_0 dv_z K(\omega_0, v_z)(v_z k_L + \hbar k_L^2/m)}{\int d\omega_0 dv_z K(\omega_0, v_z)}, \quad (7a)$$

where

$$K(\omega_0, v_z) = \frac{\exp[-(mv_z^2/2kT)]}{[\omega_L - \omega_0 - k_L \cdot v_z - (\hbar k^2/2m)]^2 + \frac{1}{4}\Gamma^2} P(\omega_0). \quad (7b)$$

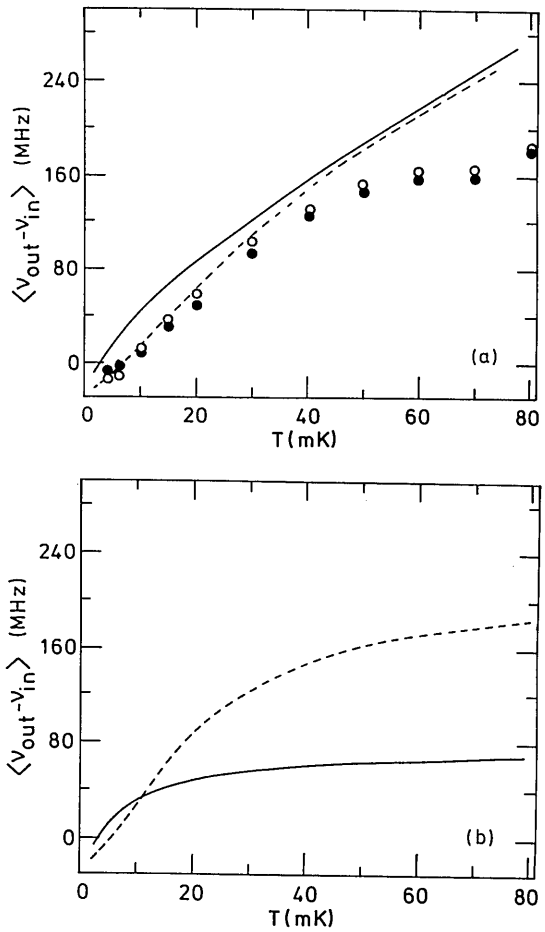

Fig. 7. Calculation of cooling in a trap. (a) Frequency shift of scattered photons calculated from Eqs. (7) for δ = 100 (solid curve) and 250 MHz (dashed curve). The circles represent the results of a computer simulation for 5×10^{10} atoms using a beam diameter of 1 mm, a bandwidth of 100 MHz, and δ = 0 without multiple scattering (●) and with multiple scattering (○). (b) The same line convention as in (a) but with the field dependence of the transition frequency neglected.

Here v_z is the component of the velocity parallel to the direction of the incoming light beam. To obtain qualitative insight we may replace the trap by a paraboloid. In that case we obtain $P(\omega_0) = (\omega_0 - \omega_m)^{1/2} \exp[-\hbar(\omega_0 - \omega_m)/2k_BT]$ for the σ_1 transition, where ω_m is the value of ω_0 at the center of the trap. The result of Eqs. (7) using this distribution function is plotted versus temperature for two values of $\delta \equiv (\omega_0 - \omega_L)$ in Fig. 7(a). For comparison we show results for the case where the field dependence of ω is neglected, i.e., when $P(\omega_0) = \delta(\omega_0 - \omega_m)$, for the corresponding value of the detuning $\delta = -\Delta/2\pi$ [Fig. 7(b)]. Positive values of $\langle \omega_s - \omega_L \rangle$ correspond to cooling, and negative ones correspond to heating. The curves for a fixed ω_0 reflect the fact that at low temperatures the cooling is more effective for a small red shift. Theory predicts[21,22] the cooling limit $T_{\min}$ to be approximately $\hbar\Gamma/2k_B$ (2.4 mK for H) for $\Delta = -\Gamma/2$ ($\delta = 50$ MHz). Solving Eqs. (7) for $P(\omega_0) = \delta(\omega_0 - \omega_m)$ actually gives slightly higher values for the optimal detuning and the base temperature ($\delta \approx 100$ MHz and $T_{\min} = 2.8$ mK). This slight discrepancy is related to the fact that the assumption that the recoil energy ϵ_{rec} is much smaller than $\hbar\Gamma$ is not strictly valid for H ($\epsilon_{\text{rec}}/k_B = 0.6$ mK and $\hbar\Gamma 2k_B = 2.4$ mK). At high temperature a larger detuning is more efficient. As can be seen by comparing Figs. 7(a) and 7(b), at higher temperatures the frequency shift of the scattered photons is larger in the case where the field dependence of ω_0 is taken into account. This is because of the self-chirping property of the trap: at higher temperature the atoms will on average be farther away from the trap center and hence in a higher field. Consequently the incoming light will appear further red shifted. This does not necessarily mean, however, that the cooling proceeds more efficiently in a trap than in the case of a homogeneous field; it should be remembered that the quantity calculated in Eqs. (7) refers only to those photons that are actually absorbed. To obtain the cooling power, $\langle \omega_s - \omega_L \rangle$ has to be multiplied by the photon flux and the total absorption. For a fixed number of particles N, the total absorption is clearly smaller in the trap case precisely because the average detuning is larger. The reason for calculating $\langle \omega_s - \omega_L \rangle$ rather than the cooling power itself is that the former quantity is independent of the number of particles for optically thin samples.

In a realistic experiment the density will be so high that the above assumption of optical transparency will no longer be correct. This has two effects: first, the source will appear to be further red shifted as the light is typically absorbed before it reaches the trap center and hence is absorbed by atoms in higher fields; second, the possibility of multiple scattering occurs. To investigate these effects we have performed a computer simulation in which photons are selected one by one from a Gaussian beam profile 1 mm wide and a Gaussian frequency distribution with a width of 100 MHz. For each scattering event the quantity $\omega_s - \omega_L$ is calculated and later averaged. The simulation was performed with 5×10^{10} atoms that were assumed to be thermally distributed in the trap. The number of atoms only enters the calculation through the local density, which in turn is related to the scattering probability at a given point. As argued above, the gas becomes more localized in the center of the our trap as it cools. Consequently the density increases from 6.7×10^{11} cm^{-3} at 80 mK to 1.3×10^{14} cm^{-3} at 7 mK. The usefulness of optical cooling in such a trap

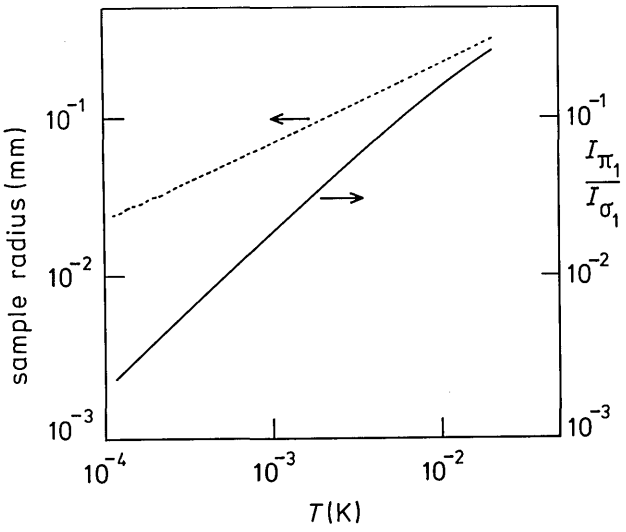

Fig. 8. Sample radius (HWHM) and the ratio of the peak intensities of the π_1 and σ_1 transitions versus temperature.

geometry lies as much in this large increase in density as in the reduction of the temperature itself. The circles in Fig. 7(a) represent the result of this simulation. As in the approximate calculation for optically thin samples, the average frequency of the incoming photons was chosen to be exactly resonant for the center of the trap. The cooling limit is found to be approximately 7.5 mK. The open circles include the effect of multiple scattering; the filled circles result when each photon is discarded after the one scattering event. At higher temperatures the cooling efficiency is slightly improved owing to the multiple scattering, and only close to the minimum temperature does a heating effect occur. The simulation revealed that in the entire temperature range the absorption is greater than 50%, even at temperatures below 10 mK, where the typical radial extent of the sample (Fig. 8) is much less than the diameter of the Ly-α beam (1 mm), reflecting the fact even in the outer layers of the gas the density is sufficient to absorb most of the light. In Section 7 we show how the large optical density may be put to use for cooling below the optical limit $T_{\min}$. By comparing the open and filled circles in Fig. 7(a), one can see that the effect of the multiple scattering turns out to be surprisingly small in spite of the fact that most of the incident light is absorbed. The reason lies in the specific geometry of the trap. The radial field gradients are much larger than the axial ones. Hence the sample acquires a pencil shape. As a consequence the opacity for radially scattered light is fairly small and most photons scatter only once. This was confirmed in the simulation, which showed that nearly all photons are scattered by the sample but only approximately 1.2–1.4 times. In contrast to the optically thin case, $\langle \omega_s - \omega_L \rangle$ is now related to the cooling rate $\dot{T}$ in a straightforward manner:

$$\hbar\langle \omega_s - \omega_L \rangle \dot{P} = m(T) k_B N \dot{T}. \tag{8}$$

Here $\dot{P}$ is the flux of incoming photons and $m(T)$ is a factor that depends on the geometry of the trap. For a paraboloid trap $m(T) = 3$, and for our trap we can approximate $m(T)$ by 4 for temperatures above 20 mK and by 3 for temperatures below 10 mK. Combining the results of the simulation with Eq. (8), we calculate that 5×10^{10} atoms can be cooled from

80 mK to less than 10 mK in approximately 10 sec. One should bear in mind that during the cooling the density increases by almost 3 orders of magnitude, thereby offering a convenient starting point for further attempts to reach BEC.

5. TRAPPING DEUTERIUM

Attempts to stabilize spin-down-polarized (D↓) or trap spin-up-polarized (D↑) deuterium in sizable concentrations have until now proved annoyingly difficult. In this Section we briefly discuss some of the problems in the context of magnetic traps. The main difficulty in trapping D is the fact that the binding energy ϵ_a of D on a surface of liquid He is approximately 2.5 times larger than for H. The consequence is that the surface coverage, which is proportional to $\exp(2\epsilon_a/k_BT)$, is enhanced by a large factor when compared with that of H. This in turn speeds up the surface recombination by a large factor. Silvera and Walraven[23] obtained densities of 10^{14} cm^{-3} of D↓, which is four orders of magnitude less than what has been obtained with H↓.[24,25] The most extensive experiments with D↓ were done by Reynolds *et al.*[26] So far our attempts to confine measurable quantities of D↑ in our trap have failed owing to this rapid surface recombination. Presumably a trap of approximately three times the depth of the present one would be required to make the confinement of D gas at wall temperature work, which would be a technical tour de force. However, an interesting alternative is to confine the gas at a temperature considerably below that of the walls. The same exponential suppression that determines τ_w [Eq. (4)] will reduce the surface recombination, allowing a substantial density to be present in the trap. For our trap a reduction of the temperature to approximately 20 mK would suffice to eliminate effectively the recombination effects. As was argued in Section 4 above, optical cooling offers the possibility of cooling to such temperatures starting with a gas of low density. Furthermore, as calculated by Koelman *et al.*,[27] the dipolar decay rate of D↑ is comparable with that of H↑ at temperatures of approximately 10 mK. Unfortunately, the ratio of the number of elastic collisions to the number of inelastic collisions (γ) is given by[27] $\gamma \sim (\mu_B B/k_B T)^{1/2}$, which is only slightly larger than unity for $B \approx 0.1$ T and $T = 10$ mK. Efficient evaporative cooling is possible only for large values of γ. However, as γ increases with decreasing temperature, the possibility of cooling to temperatures in the microkelvin region might prove feasible, perhaps at the expense of some initial loss of atoms.

6. DETECTION AND THERMOMETRY

Apart from the possibilities for optical cooling, the extreme sensitivity of detection is one of our motivations for introducing optical techniques. In our initial experiments we will measure absorption using a solar-blind phototube and an ionization chamber. The Ly-α beam will enter the cryostat from below, and the absorption will be measured at the top where the beam exits. In a later stage we plan to incorporate bolometric fluorescence measurements. The maximal time-averaged power of the VUV beam is of the order of a few microwatts. A large fraction of this light will be scattered by the sample; this fraction should be easily detectable thermally. Another application of the VUV light is thermometry. As is evident from Fig. 6(a), the Doppler and inhomogeneous broadening of the absorption profile form a measure for the temperature of the sample. At less than 10 mK, however, this method becomes of limited use as the spectral linewidth of the spectrum approaches the natural linewidth. However, at these temperatures another thermometry scheme becomes feasible. It is based on the fact that the π transitions are prohibited when the magnetic field is parallel to the direction of the incoming light. The latter condition exists on the longitudinal axis of the trap. As the temperature decreases the pencil-shaped sample becomes more localized near this axis and the π transitions become progressively weaker. This can be clearly seen by comparing the ratio of the σ_1 and π_1 transitions in Fig. 6(a). Although optical cooling is limited to temperatures above 7.5 mK, our ultimate goal is to cool the gas down to the microkelvin region. The suppression of the π intensity is well suited to perform thermometry in this temperature range. In Fig. 8 we show the calculated ratio of the peak intensities of σ_1 and π_1 for our trap as well as the radius of the sample defined by the HWHM of its radial density distribution.

7. CONCLUSIONS AND FUTURE PROSPECTS

We have argued that optical cooling of trapped H to temperatures of approximately 7.5 mK should be possible. In addition, optical techniques offer powerful nondestructive methods for detection and thermometry. However, even at densities of 10^{14} cm^{-3} the observation of quantum degenerate behavior requires a further reduction of the temperature by almost two orders of magnitude. Some form of evaporative cooling seems necessary to achieve this. In principle this evaporation can be induced by a cold finger (ideally absorbing all impinging atoms) put in the fringes of the density distribution to remove the energetic atoms preferentially. In practice this can be achieved by spatially resolved optical or microwave pumping of the atoms to a high-field-seeking hyperfine state. The advantage of such resonance methods is obvious: there is no need to insert a cold object physically into the sample space, and the cumbersome field-ramping procedures as employed in the experiments at MIT are eliminated. Microwave evaporation requires substantial modifications to the trap geometry for which we have not yet provided. Optical evaporation, however, may be readily achieved, provided that the density is sufficiently high. At $n = 10^{14}$ cm^{-3} the resonant absorption length for Ly-α is 4 μm, which is several orders of magnitude smaller than the length of the sample. This implies that the light is almost completely absorbed by the outer layers of the gas. Using a density of 10^{14} cm^{-3} we calculated that, by tuning the light to be resonant with the σ_2 transition, which decays preferentially to high-field-seeking states, atoms are removed that reside in a field corresponding to seven (at 10 mK) to five (at 100 μK) times k_BT. This allows reasonable efficient evaporative cooling to occur.

ACKNOWLEDGMENTS

We thank Raymond van Roijen for many discussions concerning the trap experiment, in which he was a major participant. We have greatly benefited from the expertise of Wim

Hogervorst on matters concerning the optical equipment. We are grateful to Steven Chu for stimulating discussions and for offering T. W. Hijmans the opportunity to spend a very educational week in his laboratory.

This research is part of the research program of the Stichting voor Fundamenteel Onderzoek der Materie, which is financially supported by the Nederlandse Organisatie voor Wetenschappelijk Onderzoek.

REFERENCES

1. I. F. Silvera and J. T. M. Walraven, in *Progress in Low Temperature Physics*, D. F. Brewer, ed. (North-Holland, Amsterdam, 1986), Vol. 10, p. 139.
2. T. J. Greytak and D. Kleppner, in *New Trends in Atomic Physics*, G. Grynberg and R. Stora, eds. (Elsevier, New York, 1984), Vol. 2, p. 1125.
3. P. D. Lett, L. P. Gould, and W. D. Phillips, *Hyperfine Interactions* **44,** 335 (1988).
4. T. W. Hijmans, O. J. Luiten, I. D. Setija, and J. T. M. Walraven, in *Proceedings of the Symposium on Spin-Polarized Quantum Systems 1988*, S. Stringari, ed. (World Scientific, Singapore, 1989), p. 275.
5. S. Chu, A. P. Mills, A. G. Yodh, K. Nagamine, Y. Miyake, and T. Kuga, Phys. Rev Lett. **60,** 103 (1988).
6. R. Hilbig and R. Wallenstein, IEEE J. Quantum Electron. **QE-15,** 1566 (1981).
7. W. A. VonDrasek, S. Okajima, and J. P. Hessler, Appl. Opt. **27,** 4057 (1988).
8. S. Chu, L. Hollberg, J. E. Bjorkholm, A. Cable, and A. Ashkin, Phys. Rev. Lett. **55,** 48 (1985).
9. V. I. Balykin, V. S. Letokhov, and V. I. Mushin, Pis'ma Zh. Eksp. Teor. Fiz. **29,** 614 (1979) [JETP Lett. **29,** 560 (1979)]; Zh. Eksp. Teor. Fiz. **78,** 1376 (1980) [Sov. Phys. JETP **51,** 692 (1980)].
10. W. D. Phillips and H. J. Metcalf, Phys. Rev. Lett. **48,** 596 (1982).
11. H. F. Hess, Phys. Rev. B **34,** 3476 (1986).
12. H. F. Hess, G. P. Kochanski, J. M. Doyle, N. Masuhara, D. Kleppner, and T. J. Greytak, Phys. Rev. Lett. **59,** 672 (1987).
13. R. van Roijen, J. J. Berkhout, S. Jaakkola, and J. T. M. Walraven, Phys. Rev. Lett. **61,** 931 (1988).
14. V. S. Bagnato, G. B. Lafyatis, A. G. Martin, E. L. Raab, R. N. Ahmad-Bitar, and D. E. Pritchard, Phys. Rev. Lett. **58,** 2194 (1987).
15. W. N. Hardy, M. Morrow, R. Jochemsen, B. W. Statt, P. R. Kubik, R. M. Marsolais, and A. J. Berlinsky, Phys. Rev. Lett. **45,** 453 (1980).
16. N. Masuhara, J. M. Doyle, J. C. Sandberg, D. Kleppner, T. J. Greytak, H. F. Hess, and G. P. Kochanski, Phys. Rev. Lett. **61,** 935 (1988).
17. A. Lagendijk, I. F. Silvera, and B. J. Verhaar, Phys. Rev. B **33,** 626 (1986).
18. H. T. C. Stoof, J. M. V. A. Koelman, and B. J. Verhaar, Phys. Rev. B **38,** 4688 (1988).
19. T. Tommila, Europhys. Lett. **2,** 789 (1986).
20. R. van Roijen, "Atomic hydrogen in a magnetic trap," Ph. D. dissertation (University of Amsterdam, 1988) (unpublished).
21. See, e.g., S. Stenholm, J. Phys. B **7,** 1235 (1974).
22. D. J. Wineland and W. M. Itano, Phys. Rev. B **20,** 1521 (1979).
23. I. F. Silvera and J. T. M. Walraven, Phys. Rev. Lett. **45,** 1268 (1980).
24. R. Sprik, J. T. M. Walraven, and I. F. Silvera, Phys. Rev. Lett. **51,** 479 (1983).
25. H. F. Hess, D. A. Bell, G. P. Kochanski, D. Kleppner, and T. J.Greytak, Phys. Rev. Lett. **51,** 483 (1983).
26. M. W. Reynolds, M. E. Hayden, and W. N. Hardy, in *Proceedings of the Third International Workshop on Spin-Polarized Quantum Systems 1988*, S. Stringari, ed. (World Scientific, Singapore, 1989), p. 236.
27. J. M. V. A. Koelman, H. T. C. Stoof, B. J. Verhaar, and J. T. M. Walraven, Phys. Rev. B **38,** 9319 (1988).